ELSEVIER

Fluid Dynamics Research 30 (2002) 127–137

FLUID DYNAMICS RESEARCH

Numerical solutions for the liquid-metal flow in a rotating cylinder with a weak transverse magnetic field

L. Martin Witkowski, J.S. Walker *

Department of Mechanical and Industrial Engineering, University of Illinois, 1206 West Green Street, Urbana, IL 61801, USA

Received 16 July 2001; received in revised form 21 September 2001; accepted 12 October 2001

Abstract

This paper treats the steady, three-dimensional, laminar flow of an electrically conducting liquid in a finite-length, insulating cylinder which rotates at a constant angular velocity about its axis. A steady, uniform, weak, transverse magnetic field produces a small deviation from a rigid-body rotation with the cylinder. This deviation consists of an axisymmetric flow, which is very similar to the classical Ekman flow for the spin-up of a cylinder, and a nonaxisymmetric flow. This paper presents numerical results for the nonaxisymmetric flow and for the ratio of the magnitude of the nonaxisymmetric flow to that of the axisymmetric flow for various values of the Reynolds number.

PACS: 47.65.a+

Keywords: Magnetohydrodynamics; Ekman flow; Asymptotic analysis; Nonaxisymmetric flow

1. Introduction

A rotating magnetic field (RMF) is often used to stir the liquid during the continuous casting of metals (Davidson and Hunt, 1987) and during the growth of single crystals of semiconductors (Dold and Benz, 1999). An RMF has an essentially constant spatial pattern which is transverse to the cylindrical liquid domain and which rotates at a constant angular velocity around the centerline of the liquid domain. For crystal-growth applications, a finite-length, electrically insulated cylinder

* Corresponding author. Tel.: +1-217-333-7979; fax: +1-217-244-6534.
E-mail address: jswalker@uiuc.edu (J.S. Walker).

PII: S0169-5983(01)00042-9

is often used to model the flow due to an RMF without the buoyant or thermocapillary convection in an actual process (Barz et al., 1997), where one end of the cylinder represents the crystal–liquid interface. If the crystal does not rotate, then the axial variation of the angular momentum created by the RMF drives a radially inward flow inside a Bödewadt layer adjacent to the crystal–liquid interface. Such a radially inward flow near the crystal–liquid interface often produces an undesirable radial nonuniformity in the crystal through the associated mass transport of additives or dopants which are rejected into the liquid during crystallization. Recently Riemann et al. (1996) grew silicon crystals by the floating-zone process with a steady, uniform, transverse magnetic field and with crystal rotations at 5–20 rpm around the centerline of the system. With a steady magnetic field and a rotating crystal, the axial variation of the angular velocity drives a radially outward flow inside a von Kármán layer adjacent to the crystal–liquid interface. As the magnetic field strength was increased in the experiments of Riemann et al. (1996), the quality of the crystals improved until the liquid motion became sufficiently nonaxisymmetric to produce undesirable qualities in the crystal.

The objectives of this paper are: (1) to quantify the deviation from axisymmetry for the flow in a rotating cylinder with a weak, steady, transverse magnetic field, and (2) to compare this deviation from axisymmetry to that for a fixed cylinder with an RMF. If the magnetic field is sufficiently strong that inertial effects, including the Coriolis acceleration, are negligible, then the flow in a rotating cylinder with a steady, transverse magnetic field is identical to the flow in a fixed cylinder with an RMF (Alemany and Moreau, 1977). Unfortunately crystals grown with strong transverse magnetic fields have undesirable properties due to the large deviation from axisymmetry in the liquid motion (Hoshi et al., 1985). Therefore, the objective is to apply a rotating or steady magnetic field which is strong enough to produce a significant forced convection, but which is weak enough to produce only a small deviation from an axisymmetric flow.

Two important parameters are the interaction parameter $N=\sigma B^2/\rho\omega$ and the Reynolds number $Re=\rho\omega R^2/\mu$, where B is the magnetic flux density of the steady magnetic field, ω and R are the angular velocity and inside radius of the cylinder, and σ, ρ and μ are the electrical conductivity, density and dynamic viscosity of the liquid. In order to estimate the magnitudes of these and other parameters, we use an example with the properties of molten silicon (Sabhapathy and Salcudean, 1991), $R=2.5$ cm corresponding to the experiments of Riemann et al. (1996), $\omega=1.047$ rad/ s (10 rpm) and $B=10$ mT. Then $N=0.0378$ and $Re=2350$. Therefore, we use an asymptotic analysis for $N\ll 1$. The $O(1)$ term in the asymptotic solution is simply a rigid-body rotation of the liquid with the cylinder, and the $O(N)$ term is the small, three-dimensional deviation from this rigid-body rotation due to the steady, weak, transverse magnetic field, $B\hat{\mathbf{x}}$, where $\hat{\mathbf{x}}=\cos\theta\hat{\mathbf{r}}-\sin\theta\hat{\theta}$ is a unit vector which is parallel to the $\theta=0$ plane, while $\hat{\mathbf{r}},\hat{\theta},\hat{\boldsymbol{z}}$ are unit vectors for the cylindrical coordinates r,θ,z, with the z-axis along the vertical centerline. We call the azimuthal average of the $O(N)$ three-dimensional flow the axisymmetric flow and the rest of $O(N)$ flow the nonaxisymmetric flow.

2. Problem formulation

In addition to the uniform magnetic field produced by external magnets, there is an induced magnetic field produced by the electric current in the melt. The characteristic ratio of the induced magnetic field to the externally applied field is the magnetic Reynolds number $R_m=\mu_p\sigma\omega R^2$,

where μ_p is the melt's magnetic permeability. For our example, $R_m = 0.0008$, so that the induced magnetic field can be neglected.

The dimensionless equations governing the steady incompressible flow are

$$(\mathbf{v} \cdot \nabla)\mathbf{v} = -\nabla p + N(\mathbf{j} \times \hat{\mathbf{x}}) + Re^{-1}\nabla^2\mathbf{v}, \tag{1a}$$

$$\nabla \cdot \mathbf{v} = 0, \tag{1b}$$

$$\mathbf{j} = -\nabla\phi + \mathbf{v} \times \hat{\mathbf{x}}, \tag{1c}$$

$$\nabla \cdot \mathbf{j} = 0, \tag{1d}$$

where $\mathbf{v}$, p, $\mathbf{j}$ and ϕ are the melt velocity, pressure, electric current density and electric potential function, normalized by ωR, $\rho\omega^2R^2$, $\sigma\omega RB$ and $\omega R^2 B$, respectively, while $\hat{x}$ is the dimensionless magnetic field. Eq. (1a) is the Navier–Stokes equation and Eq. (1c) is Ohm's law, while Eqs. (1b) and (1d) guarantee conservation of mass and electric charge. The boundary conditions are

$$\mathbf{v} = r\hat{\theta}, \tag{2a}$$

$$j_z = 0 \quad \text{at } z = \pm h, \tag{2b}$$

$$\mathbf{v} = \hat{\theta}, \tag{2c}$$

$$j_r = 0 \quad \text{at } r = 1, \tag{2d}$$

where r and z are normalized by R, and h is the ratio of the cylinder's length to its diameter. Since the flow is symmetric about $z = 0$, we need only treat $z \geqslant 0$.

For $N \ll 1$,

$$\mathbf{v} = r\hat{\theta} + N[\mathbf{v}_a(r,z) + \cos(2\theta)\mathbf{v}_c(r,z) + \sin(2\theta)\mathbf{v}_s(r,z)], \tag{3a}$$

$$p = \frac{r^2}{2} + N[p_a(r,z) + \cos(2\theta)\,p_c(r,z) + \sin(2\theta)\,p_s(r,z)], \tag{3b}$$

both neglecting $O(N^2)$ terms. With only the rigid-body rotation in Ohm's law,

$$\phi = \cos\theta\phi_c(r,z), \tag{4a}$$

$$\mathbf{j} = \cos\theta j_{rc}(r,z)\hat{\mathbf{r}} + \sin\theta j_{\theta s}(r,z)\hat{\theta} + \cos\theta j_{zc}(r,z)\hat{\mathbf{z}}, \tag{4b}$$

both neglecting $O(N)$ terms. Eq. (1c) gives

$$j_{rc} = -\frac{\partial\phi_c}{\partial r}, \tag{5a}$$

$$j_{\theta s} = \frac{\phi_c}{r}, \tag{5b}$$

$$j_{zc} = -\frac{\partial\phi_c}{\partial z} - r. \tag{5c}$$

The solution of Eqs. (1d), (2b), (2d) and (5), neglecting $O(N)$ terms is

$$\phi_c = -2\sum_{n=1}^{\infty} \frac{J_1(\lambda_n r)\sin h(\lambda_n z)}{\lambda_n(\lambda_n^2 - 1)J_1(\lambda_n)\cos h(\lambda_n h)}, \tag{6}$$

where J_k are the Bessel functions of the first kind and kth order, while λ_n are the roots of $\lambda_n J_0(\lambda_n) - J_1(\lambda_n) = 0$.

The equations governing the axisymmetric flow are

$$-2v_{\theta a} = -\frac{\partial p_a}{\partial r} + Re^{-1}\left[\nabla^2 v_{ra} - \frac{v_{ra}}{r^2}\right], \tag{7a}$$

$$2v_{ra} = -\frac{1}{2}\left[\frac{\partial \phi_c}{\partial z} + r\right] + Re^{-1}\left[\nabla^2 v_{\theta a} - \frac{v_{\theta a}}{r^2}\right], \tag{7b}$$

$$0 = -\frac{\partial p_a}{\partial z} + Re^{-1}\nabla^2 v_{za}, \tag{7c}$$

$$\frac{1}{r}\frac{\partial}{\partial r}(r v_{ra}) + \frac{\partial v_{za}}{\partial z} = 0, \tag{7d}$$

where

$$\nabla^2 = \frac{\partial^2}{\partial r^2} + \frac{1}{r}\frac{\partial}{\partial r} + \frac{\partial^2}{\partial z^2}. \tag{7e}$$

The boundary conditions are that $\mathbf{v}_a = 0$ at $r = 1$ and at $z = h$. We introduce a meridional flow stream function $\psi(r,z)$, so that

$$v_{ra} = \frac{1}{r}\frac{\partial \psi}{\partial z}, \tag{8a}$$

$$v_{za} = -\frac{1}{r}\frac{\partial \psi}{\partial r} \tag{8b}$$

and we cross-differentiate Eqs. (7a) and (7c) in order to eliminate p_a. This gives two coupled linear equations governing ψ, $v_{\theta a}$ which were solved numerically using a Chebyshev spectral collocation method.

The equations governing the nonaxisymmetric flow are

$$2v_{rs} - 2v_{\theta c} = -\frac{\partial p_c}{\partial r} + Re^{-1}\left[\nabla^2 v_{rc} - \frac{5}{r^2}v_{rc} - \frac{4}{r^2}v_{\theta s}\right], \tag{9a}$$

$$-2v_{rc} - 2v_{\theta s} = -\frac{\partial p_s}{\partial r} - \frac{1}{2}\left[\frac{\partial \phi_c}{\partial z} + r\right] + Re^{-1}\left[\nabla^2 v_{rs} - \frac{5}{r^2}v_{rs} + \frac{4}{r^2}v_{\theta c}\right], \tag{9b}$$

$$2v_{rc} + 2v_{\theta s} = -\frac{2}{r}p_s - \frac{1}{2}\left[\frac{\partial \phi_c}{\partial z} + r\right] + Re^{-1}\left[\nabla^2 v_{\theta c} - \frac{5}{r^2}v_{\theta c} + \frac{4}{r^2}v_{rs}\right], \tag{9c}$$

$$2v_{rs} - 2v_{\theta c} = \frac{2}{r}p_c + Re^{-1}\left[\nabla^2 v_{\theta s} - \frac{5}{r^2}v_{\theta s} - \frac{4}{r^2}v_{rc}\right], \tag{9d}$$

$$2v_{zs} = -\frac{\partial p_c}{\partial z} + Re^{-1}\left[\nabla^2 v_{zc} - \frac{4}{r^2}v_{zc}\right], \tag{9e}$$

$$-2v_{zc} = -\frac{\partial p_s}{\partial z} + \frac{1}{2}\left[\frac{\partial \phi_c}{\partial r} - \frac{\phi_c}{r}\right] + Re^{-1}\left[\nabla^2 v_{zs} - \frac{4}{r^2}v_{zs}\right], \tag{9f}$$

$$\frac{1}{r}\frac{\partial}{\partial r}(rv_{rc}) + \frac{2}{r}v_{\theta s} + \frac{\partial v_{zc}}{\partial z} = 0, \tag{9g}$$

$$\frac{1}{r}\frac{\partial}{\partial r}(rv_{rs}) - \frac{2}{r}v_{\theta c} + \frac{\partial v_{zs}}{\partial z} = 0. \tag{9h}$$

The boundary conditions are that $\mathbf{v}_c = \mathbf{v}_s = 0$ at $r = 1$ and at $z = h$. The Taylor series for v_{rc}, v_{rs}, $v_{\theta c}$ and $v_{\theta s}$ have only odd powers of r, while those for v_{zc}, v_{zs}, p_c and p_s have only even powers starting with r^2. We used Eqs. (9g) and (9h) to eliminate $v_{\theta c}$ and $v_{\theta s}$ from the other equations and from the boundary conditions. We then used Eqs. (9c) and (9d) to eliminate p_c and p_s from Eqs. (9a), (9b), (9e) and (9f). This gives four coupled linear equations governing v_{rc}, v_{rs}, v_{zc} and v_{zs}, which were solved numerically using the same Chebyshev spectral collocation method.

3. Results

For all the results presented here, $h = 1$. For the axisymmetric flow and for $Re = 2000$, the meridional-flow streamlines and the contours of constant $v_{\theta a}$ are presented in Fig. 1. The present axisymmetric flow is very close to the classical Ekman flow arising when the angular velocity of a liquid-filled cylinder is increased from ω to $\omega(1 + \varepsilon)$ with $\varepsilon \gg 1$ (Greenspan, 1968). During the transient differential spin-up in the Ekman problem, the axial variation of v_θ drives a radially outward flow near each end of the cylinder, and the resulting Ekman pumping pulls liquid with less azimuthal velocity from the central part of the liquid. The flow is completed by axial flow away from the ends near the vertical wall at $r = 1$. Here we have a steady Ekman flow with a balance between the addition of angular momentum due to shear stresses at the cylinder walls and the removal of angular momentum by the EM body force opposing the azimuthal melt motion. Since the present axisymmetric flow is very similar to the classical Ekman flow, the results for the axisymmetric flow are only presented here in order to quantify the relationship between the axisymmetric and nonaxisymmetric flows.

The contours of constant values of v_{rc}, v_{rs}, $v_{\theta c}$, $v_{\theta s}$ v_{zc}, and v_{zs} for $Re = 2000$ are presented in Fig. 2. All the functions of r and z could be introduced into Eq. (3a) to obtain the complete solution for the $O(N)$ three-dimensional perturbation of the rigid-body rotation with the cylinder. However, it is difficult to gain physical insights into this complex three-dimensional flow. For physical insights, it is better to consider the $O(N)$ perturbation to be the superposition of the axisymmetric Ekman flow in Fig. 1 and two separate nonaxisymmetric flows. The first nonaxisymmetric flow is

$$v_{rc}\cos(2\theta)\hat{\mathbf{r}} + v_{\theta s}\sin(2\theta)\hat{\theta} + v_{zc}\cos(2\theta)\hat{\mathbf{z}}, \tag{10}$$

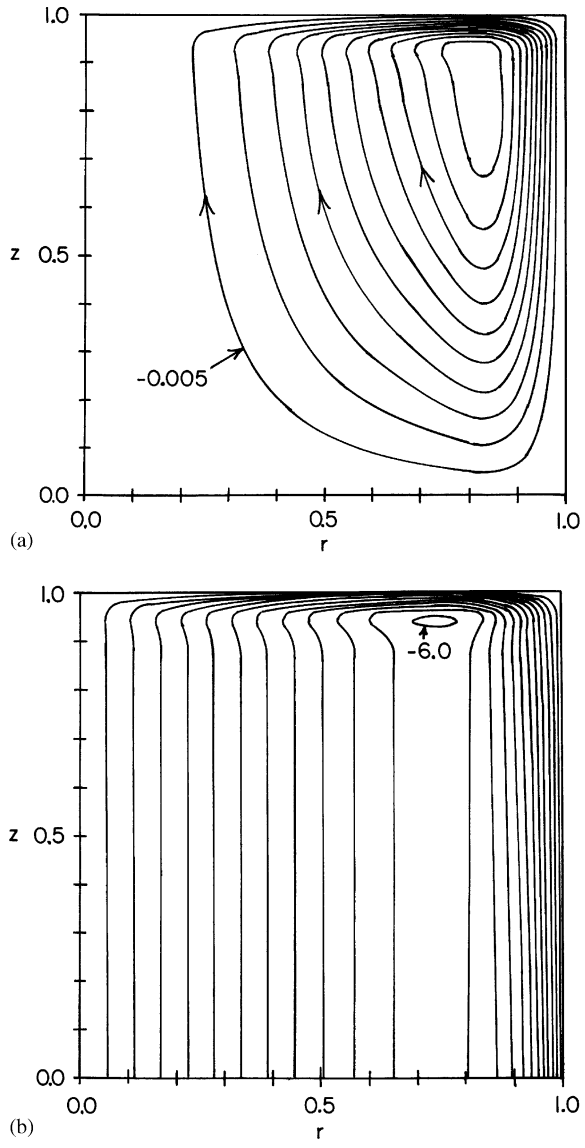

Fig. 1. Axisymmetric flow for $Re = 2000$. (a) Meridional flow streamlines $\psi = -0.005k$ for $k = 1$ to 10. (b) Contours of constant $v_{\theta a} = -0.5k$ for $k = 1$ to 12.

where the values of v_{rc}, $v_{\theta s}$ and v_{zc} are presented in Fig. 2a, d and e, respectively. This nonaxisymmetric flow represents a circulation between the $\theta = 0$ and $\pi/2$ planes, with identical reflected circulations in the other three quadrants. At the $\theta = \pi/4$ plane, there is azimuthal flow in the $+\theta$ and $-\theta$ directions above and below the $v_{\theta s} = 0$ contour in Fig. 2d, which runs from $z = 0.7$ at $r = 0$ to $z = 0.9$ at $r = 1$. For this circulation, the closed streamline through $r = 0.6$, $\theta = \pi/4$ and $z = 0.9$ is shown as loop 1 in Fig. 3. For $0 \leqslant \theta \leqslant \pi/4$, the flow crossing the $\theta = \pi/4$ plane in the

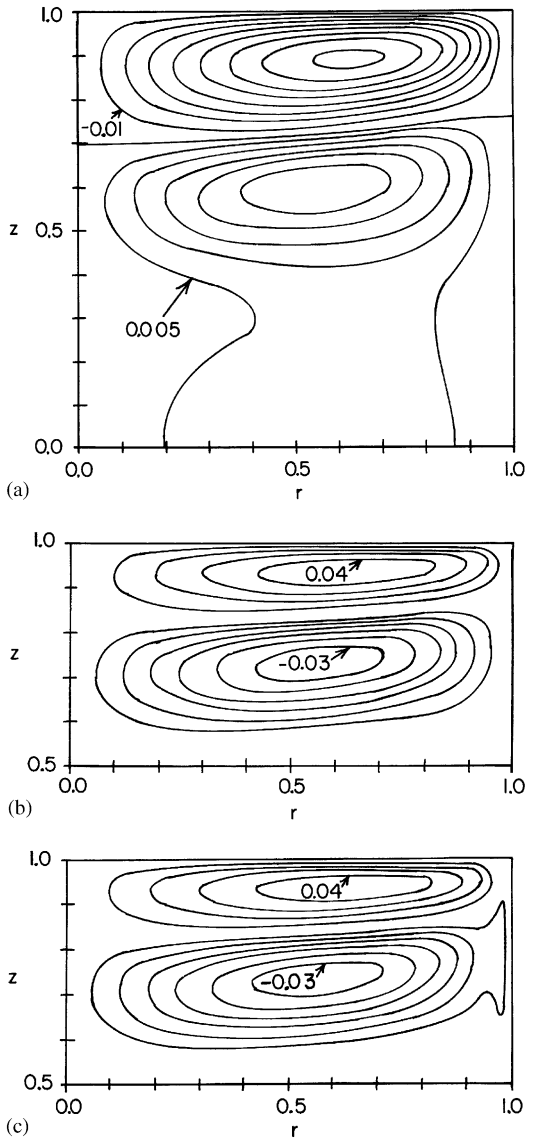

Fig. 2. Contours of the nonaxisymmetric flow velocity components for $Re = 2000$. (a) $v_{rc} = -0.01k$ for $k = 0$ to 8 and $v_{rc} = 0.005k$ for $k = 1$ to 5. (b) $v_{rs} = -0.005k$ for $k = 1$ to 6 and $v_{rs} = 0.01k$ for $k = 1$ to 4. (c) $v_{\theta c} = -0.005k$ for $k = 1$ to 6 and $v_{\theta c} = 0.01k$ for $k = 1$ to 4. (d) $v_{\theta s} = -0.005k$ for $k = 0$ to 5 and $v_{\theta s} = 0.01k$ for $k = 1$ to 8. (e) $v_{zc} = 0.01k$ for $k = 1$ to 7. (f) $v_{zs} = -0.005k$ for $k = 1$ to 7.

$-\theta$ direction: (1) turns to flow radially outward with the positive values of v_{rc} for $z < 0.725$ in Fig. 2a, (2) then turns to flow axially toward $z = h$ with the positive values of v_{zc} in Fig. 2e, (3) then flows radially inward with the negative values of v_{rc} for $z > 0.725$ in Fig. 2a, and (4) finally turns to cross the $\theta = \pi/4$ plane in the $+\theta$ direction as the positive values of $v_{\theta s}$ in Fig. 2d. Similarly for $\pi/4 \leqslant \theta \leqslant \pi/2$, the flow crossing the $\theta = \pi/4$ plane in the $+\theta$ direction first flows radially outward,

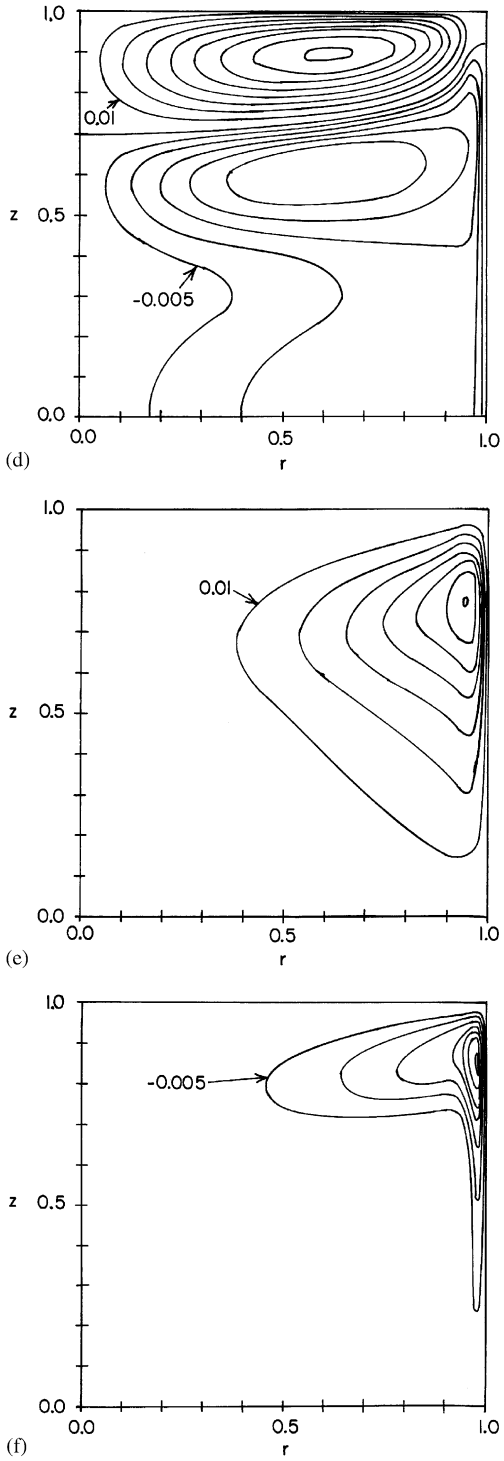

Fig. 2. (*Continued*).

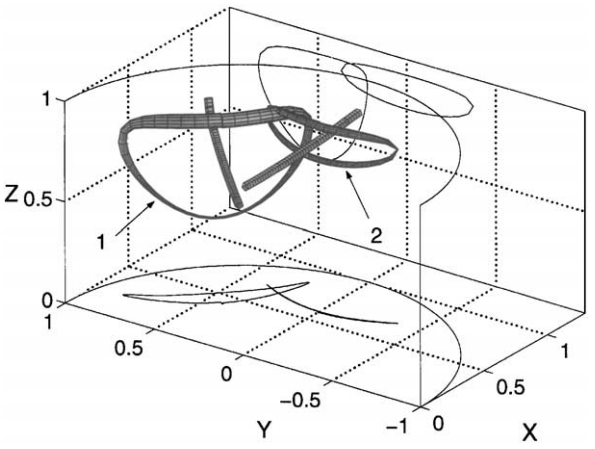

Fig. 3. Two closed toroidal surfaces whose center lines are closed streamlines and whose radius is proportional to the magnitude of the velocity. Loop 1 is the streamline through $r = 0.6$, $\theta = \pi/4$, $z = 0.9$ for the circulation associated with $v_{rc}, v_{\theta s}, v_{zc}$, while the velocity for this circulation is zero along the line in the $\theta = \pi/4$ plane. Loop 2 is the closed streamline through $r = 0.6$, $\theta = 0$, $z = 0.92$ for the circulation associated with $v_{rs}, v_{\theta c}, v_{zs}$, while the velocity for this circulation is zero along the line in the $\theta = 0$ plane. The projections of both streamlines onto a horizontal plane and onto a vertical plane are also shown.

then axially downward, then radially inward before turning to complete this circulation. The second nonaxisymmetric flow is

$$v_{rs}\sin(2\theta)\hat{\mathbf{r}} + v_{\theta c}\cos(2\theta)\hat{\theta} + v_{zs}\sin(2\theta)\hat{\mathbf{z}}, \tag{11}$$

where v_{rs}, $v_{\theta c}$ and v_{zs} are presented in Figs. 2b, c and f, respectively. This nonaxisymmetric flow represents a circulation which is very similar to that for the first nonaxisymmetric flow, except that the circulation is shifted to the quadrant $-\pi/4 \leqslant \theta \leqslant \pi/4$, again with identical reflected circulations in the other three quadrants. For this circulation, the streamline through $r = 0.6$, $\theta = 0$, and $z = 0.92$ is shown as loop 2 in Fig. 3.

For crystal-growth processes, the primary concern is whether the three-dimensional flow creates deviations from axisymmetry in the concentrations of additives or dopants which have nonuniform distributions in the liquid because they are rejected into the liquid during crystallization. Therefore, the key quantities are the deviations from axisymmetry in v_r and v_z. For the present rotating cylinder with a steady magnetic field, both the axisymmetric and nonaxisymmetric components of v_r and v_z are $O(N)$. From Figs. 1 and 2, the maximum values of $(v_{rc}^2 + v_{rs}^2)^{1/2}/v_{ra}$ and of $(v_{zc}^2 + v_{zs}^2)^{1/2}/v_{za}$ are 0.0522 and 0.139, respectively, for $Re = 2000$. Therefore, for our example, there are significant deviations from axisymmetry in the radial and axial velocities.

4. Concluding remarks

A primary purpose of this paper is to compare the deviations from axisymmetry in the radial and axial velocities (1) for a rotating cylinder with a steady, transverse magnetic field and (2) for a fixed cylinder with a RMF. The first part of this comparison involves the orders of magnitude of the velocities for small values of the interaction parameter N. For a rotating cylinder with a steady,

transverse magnetic field, (1) the nonaxisymmetric flow is limited to $O(N)$ by inertial effects because the perturbation velocity is reversed four times during each revolution of a fluid particle with the rigid-body rotation, and (2) the axisymmetric flow is limited to $O(N)$ by the Coriolis acceleration because any radial perturbation velocity convects the angular momentum of the rigid-body rotation, creating a large change in the perturbation azimuthal velocity. For a fixed cylinder with an RMF, the key parameters are N and Re based on the angular velocity ω of the RMF. The main difference arises from the fact that the fluid is stagnant with an RMF for $N = 0$. Again the nonaxisymmetric flow is limited to $O(N)$ because it reverses direction four times during each rotation of the RMF, but, without the Coriolis acceleration associated with the rigid-body rotation, the axisymmetric flow grows to $O(N^{1/2})$ (Martin Witkowski et al., 1999). Thus for the rotating cylinder with a steady magnetic field, the ratio of the nonaxisymmetric radial or axial velocity to the corresponding axisymmetric velocity is $O(1)$, i.e., independent of N for small values of N. On the other hand, the same ratios for a fixed cylinder with an RMF are $O(N^{1/2})$, so that they become smaller as N becomes smaller.

For our example, $N = 0.0378$, so that the deviation from axisymmetry for a rotating cylinder with a steady field is not dramatically larger than that for a fixed cylinder with an RMF. However, the second part of this comparison involves the differences between the values of N for practical crystal-growth applications. For our example of a rotating cylinder with a steady transverse magnetic field, we used $B = 10$ mT and $\omega = 1.047$rad/s (10 rpm), leading to $N = 0.0378$. For crystal-growth processes, it is generally not practical to rotate the crystal at an angular velocity above 20 rpm ($\omega = 2.094$ rad/s), while a weaker magnetic field would not lead to any benefits, so that N cannot be reduced. On the other hand, for a fixed or slowly rotating crystal with an RMF, typical angular velocities of the RMF are 120π rad/s (60 Hz) and 800π rad/s (400 Hz). For our silicon example with $B = 10$ mT, N is 0.000105 and 0.0000157 for 60 and 400 Hz, respectively. For such small values of N, the deviations from axisymmetry for a fixed cylinder with an RMF are extremely small. On the other hand, for a rotating cylinder with a steady, transverse magnetic field, the ratio of the nonaxisymmetric to axisymmetric velocity would still be 0.0522 or 0.139 for the radial or axial velocity, respectively, even if we could achieve such small values of N for the rotating cylinder.

Acknowledgements

This research was supported by the National Aeronautics and Space Administration under Grant No. NAG8-1453 and NAG8-1705. The calculations were performed on a workstation donated by the International Business Machines Corporation.

References

Alemany, A., Moreau, R., 1977. Ecoulement d'un fluide conducteur de l'électricité en présence d'un champ magnétique tournant. J. de Mécanique 16, 625–646.

Barz, R.U., Gerbeth, G., Wunderwald, U., Buhrig, E., Gelfgat, Y.M., 1997. Modelling of the isothermal melt flow due to rotating magnetic fields in crystal growth. J. Crystal Growth 180, 410–421.

Davidson, P.A., Hunt, J.C.R., 1987. Swirling recirculating flow in a liquid metal column generated by a rotating magnetic field. J. Fluid Mech. 185, 67–106.

Dold, P., Benz, K.W., 1999. Rotating magnetic field: fluid flow and crystal growth applications. Progr. Crystal Growth Characterization Mater. 38, 7–37.

Greenspan, H.P., 1968. The Theory of Rotating Fluids. Cambridge University Press, Cambridge.

Hoshi, K., Isawa, N., Suzuki, T., Ohkubo, Y., 1985. Czochralski silicon crystals grown in a transverse magnetic field. J. Electrochem. Soc., Solid State Sci. Technol. 132, 693–700.

Martin Witkowski, L., Walker, J.S., Marty, P., 1999. Nonaxisymmetric flow in a finite-length cylinder with a rotating magnetic field. Phys. Fluids 11, 1821–1826.

Riemann, H., Lüdge, A., Hallmann, B., Turschner, T., 1996. Growth of floating zone (FZ) silicon crystals under the influence of a transversal magnetic field. Proc. Electrochem. Soc. 96–13, 49–57.

Sabhapathy, P., Salcudean, M.E., 1991. Numerical study of Czochralski growth of silicon in an axisymmetric magnetic field. J. Crystal Growth 113, 164–180.